Nanoscale
Advances

ROYAL SOCIETY
OF CHEMISTRY

MINIREVIEW
Mohammad H. Malakooti, Carmel Majidi *et al.*
Liquid metal nanocomposites

NCNST

Liquid metal nanocomposites

Mohammad H. Malakooti, [ID] *[a] Michael R. Bockstaller,[b] Krzysztof Matyjaszewski[c] and Carmel Majidi [ID] *[bd]

Liquid metal (LM) has attracted tremendous interest over the past decade for its enabling combination of high electrical and thermal conductivity and low mechanical compliance and viscosity. Efforts to harness LM in electronics, robotics, and biomedical applications have largely involved methods to encapsulate the liquid so that it can support functionality without leaking or smearing. In recent years, there has been increasing interest in LM "nanocomposites" in which either liquid metal is mixed with metallic nanoparticles or nanoscale droplets of liquid metal are suspended within a soft polymer matrix. Both of these material systems represent an important step towards utilizing liquid metal for breakthrough applications. In this minireview, we present a brief overview of recent progress over the past few years in methods to synthesize LM nanomaterials and utilize them as transducers for sensing, actuation, and energy harvesting. In particular, we focus on techniques for stable synthesis of LM nanodroplets, suspension of nanodroplets within various matrix materials, and methods for incorporating metallic nanoparticles within an LM matrix.

Introduction

Metals that are liquid at room temperature have the potential for transformative impact in applications that depend on combining high electrical or thermal conductivity with extreme mechanical compliance and deformability.[1] Over the past decade, liquid metal (LM) alloys like eutectic gallium–indium (EGaIn) and gallium–indium–tin (Galinstan) have been shown to provide a unique functional role in applications ranging from soft and stretchable "second skin" electronics for wearable sensing[2–4] to stimuli-responsive actuators capable of field-controlled motion and reversible shape change[5–7] and intracellular drug delivery.[8] Such applications of LM in wearable electronics, soft robotics, and nanomedicine have largely focused on ways to encapsulate the liquid so that it can remain intact during interaction with other materials. While the use of microfluidic channels of liquid metal encapsulated in soft

[a]Department of Mechanical Engineering, University of Washington, Seattle, WA 91895, USA. E-mail: malakoot@uw.edu

[b]Department of Materials Science & Engineering, Carnegie Mellon University, Pittsburgh, PA 15213, USA. E-mail: cmajidi@andrew.cmu.edu

[c]Department of Chemistry, Carnegie Mellon University, Pittsburgh, PA 15213, USA

[d]Department of Mechanical Engineering, Carnegie Mellon University, Pittsburgh, PA 15213, USA

Mohammad H. Malakooti is an Assistant Professor of Mechanical Engineering at the University of Washington. He leads a research group dedicated to creating materials that match the extraordinary adaptability, rich multi-functionality, and embodied intelligence of natural material systems by bridging the gap between nanoscale engineering and system-level functionality. He received his PhD at the University of Florida, had a postdoctoral fellowship at the University of Michigan, and was a research scientist at Carnegie Mellon University, where he worked with Prof. Carmel Majidi.

Michael R. Bockstaller is Professor in the Department of Materials Science and Engineering at Carnegie Mellon University. His research is concerned with structure formation and structure–property relations in polymer and polymer hybrid materials. He received his diploma in Chemistry from the Technical University of Karlsruhe (Germany) and his Dr rer. nat. (Sc.D.) in Physical Chemistry from the Johannes Gutenberg University (Mainz, Germany). He is a fellow of the American Physical Society and the Alexander von Humboldt foundation.

elastomer remains a popular approach,[2,4] there has been increasing interest in material systems composed of a suspension of LM droplets that are either isolated from each other or connected to form electrically conductive pathways.[9,10] In recent years, these latter efforts have merged with practices in LM-based nanotechnology[11] to enable a new domain of research on the topic of *liquid metal nanocomposites*.

LM nanocomposites represent material systems in which LM alloys like EGaIn or Galinstan are either suspended as nanoscale droplets within a soft polymer matrix or mixed with metallic nanoparticles to form a biphasic composition in which the LM functions as the continuous matrix phase. In either case, LM nanocomposites represent a potential paradigm-shift in how we tailor the electrical, dielectric, and thermal properties of soft materials. Historically, efforts to alter such properties in soft materials have typically focused on particle-filled composites with rigid metal, ceramic nanoparticles, or carbon allotropes. However, such filler materials lead to increased stiffness and mechanical hysteresis, especially at the high concentrations required for percolation and electrical conductivity. While acceptable for some applications, such a trade-off is greatly limiting for emerging technologies in computing, robotics, and medicine that require mechanical compliance matching with soft materials and biological tissue. In this respect, replacing rigid filler with LM nanodroplets can significantly broaden the range of applications in which nanocomposite materials can be used.

Here, we review recent advances in methods to synthesize LM nanocomposites and their application for soft-matter sensing, actuation, and energy harvesting. We begin with summarizing technical background and progress in methods to synthesize nanoscale LM droplets that can form stable suspensions within solvents. Next, we cover recent developments in LM-polymer nanocomposites that are comprised of LM nanodroplets embedded within a soft, elastomeric medium. Lastly, we discuss parallel efforts in creating material systems in which rigid metallic nanoparticles are embedded within bulk

liquid metal. Such "biphasic" compositions result in a paste-like substance that can be engineered to have intriguing electrical, magnetic, and stimuli-responsive properties.

LM nanodroplet synthesis

Typically, the first step in creating LM nanocomposites is to prepare a dispersion of liquid metal nanodroplets within a solvent.[12] Over the past decade, researchers have developed techniques to create stabilized LM nanodroplets for a range of droplet sizes, size distributions (dispersity), surfactants, and solvents. Earlier research focused on ultrasonication of EGaIn with 1-dodecanethiol (C12) and 3-mercapto-*N*-nonylpropionamide (1ATC9).[13] Droplet stabilization was attributed to chemical reaction of sulfur atoms with the surface of the EGaIn droplets as well as surface oxidation (Fig. 1a). Yamaguchi *et al.*[14] likewise found that C12SH and surface oxidation had a central role in regulating the stability of LM nanodroplets synthesized with ultrasonication. In their study, Ga nanodroplets with an average diameter of 35 nm were synthesized (Fig. 1b). They also observed that reaction temperature in the range of 20 °C to 50 °C had an influence on mean droplet size and distribution. Ga nanodroplets prepared by ultrasonication at 50 °C had a larger mean diameter ($\sim$60 nm), which is $\sim$1.7 times of that for nanoparticles synthesized at 20 °C. However, the size of $\sim$35 nm Ga nanoparticles synthesized at 20 °C did not increase by elevating the temperature to 50 °C after the synthesis.

LM nanodroplets synthesized with this method have been used to create stretchable electronic circuits through pressure-controlled "sintering" of a film of droplets deposited on a soft elastomeric substrate as shown in Fig. 1c.[15,16] For example, Boley *et al.*[15] performed ultrasonication of EGaIn in ethanol and compared the ease of sintering with droplets synthesized with or without 1ATC9. In this way, they could examine the functional role of a thiol-capped self-assembled monolayer *versus* gallium oxide coating in resisting or facilitating mechanical

Krzysztof Matyjaszewski is the J. C. Warner University Professor of Natural Sciences and Director of the Center for Macromolecular Engineering in the Mellon College of Science at Carnegie Mellon University. He is an internationally recognized polymer chemist who is highly regarded for his vision, his leadership in education and his many collaborative research efforts that have yielded significant innovations in polymer chemistry. He is perhaps best known for the discovery of atom transfer radical polymerization (ATRP), a novel method of polymer synthesis that has revolutionized the way macromolecules are made.

Carmel Majidi is the Clarence H. Adamson Professor of Mechanical Engineering at Carnegie Mellon University. He leads the Soft Machines Lab, which develops novel materials architectures, theoretical models, and fabrication methods for soft multifunctional composites and microfluidics. Professor Majidi's research contributes to the fields of soft bioinspired robotics, wearable computing, and mechanics of soft matter. Prior to joining Carnegie Mellon University, he had postdoctoral fellowships at Princeton and Harvard Universities. He received his B.S. degree from Cornell University and M.S. and PhD degrees from UC Berkeley.
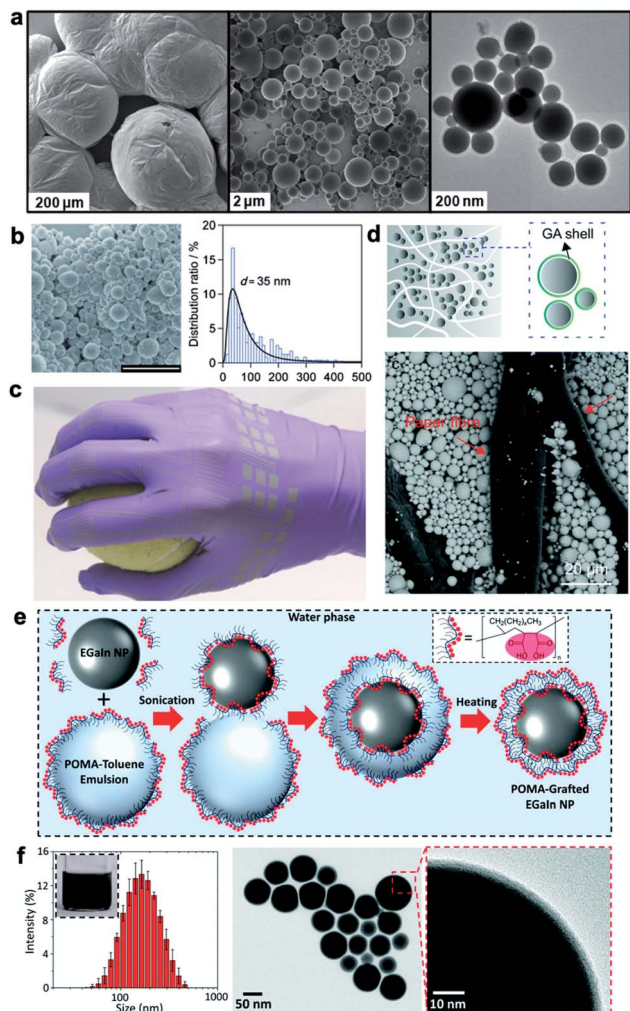
Fig. 1 Synthesis of LM nanodroplets. (a) liquid-phase eutectic gallium–indium (EGaIn) alloy nanoparticles prepared by molecular self-assembly and assisted by sonication. Reproduced with permission,[13] copyright 2011, American Chemical Society. (b) SEM image of Ga nanoparticles prepared by 40% power ultrasonication at 20 °C for 120 min (scale bar: 1 μm) with particle size distribution. Reproduced with permission,[14] copyright 2015, Wiley-VCH. (c) Human hand wearing inkjet functionalized nitrile glove with arrays of strain gauges, intricate wiring, and contact pads comprised of EGaIn nanoparticles. Reproduced with permission,[15] copyright 2015, Wiley-VCH. (d) Top: schematic illustration of the impregnation process of Ga particles stabilized with gallic acid embedded into a paper membrane – bottom: SEM image shows the successful incorporation Ga particles in the membrane, reproduced with permission,[24] copyright 2019, Royal Society of Chemistry. (e) Schematic depicting the mechanism leading to the production of stable liquid metal nanoparticles with poly(1-octadecene-*alt*-maleic anhydride) (POMA). (f) Left: hydrodynamic size distribution of the POMA grafted EGaIn NPs; the inset shows the NP colloidal suspension. Center-/right: TEM images of the produced nanoparticles. Reproduced with permission,[25] copyright 2019, Royal Society of Chemistry.

sintering. More recently, laser sintering was introduced as a remote activation method to rupture the oxide skin of LM droplets and transform nonconductive LM nanoparticle films into electrically conductive patterns. This method is particularly suitable for small (<70 nm) LM droplets.[17,18] Finkenauer *et al.*[19]

explored the role of surfactants in nanodroplet synthesis in even greater detail by investigating droplet mean size, size distribution, and yield for a variety of surfactants with thiol, amine, and carboxylic acid functionality. Among these, they found that thiol-based surfactants, in particular 1-octadecanethiol, were the most effective for synthesizing LM nanodroplets with relatively high yield and low dispersity compared to surfactant-free ultrasonication in ethanol. Such results are consistent with the findings of Farrell *et al.*,[20] who showed that various thiols had different influences on moderating gallium oxide growth and claimed that these modifications can be captured by the Cabrera–Mott oxidation model. More recently, Morris *et al.* have explored various chemical treatments to synthesize EGaIn nanodroplets with varied oxide shell thickness (between 1.28 and 4.46 nm) while maintain an average diameter of ∼50 nm for EGaIn nanodroplets.[21] They showed that the stiffness of LM nanoparticles increases up to two orders of magnitude as the shell thickness increases. This implies the critical role of the oxide shell on structural and functional properties of LM nanocomposites. In addition to chemical treatment, physical surface modification like nanotexturing of LM droplets[22,23] can be utilized to further engineer the surface of LM droplets and tune the interface properties for LM nanocomposites.

Alternatively, immersion mixing can be utilized to synthesize LM nanoparticles. In an earlier study by Tevis *et al.*,[26] EGaIn nano-/microparticles (∼6 nm to ∼10 μm) were synthesized by mixing bulk EGaIn in an acidic carrier fluid. More recently, the researchers applied this method to synthesis of undercooled LM micro-/nanoparticles such as Field's metal (eutectic bismuth–indium–tin) and eutectic bismuth–tin droplets.[27,28] This synthesis method has been further extended by immersion mixing of LM droplets in polymers for LM polymer composites[29] and by incorporation of metallic fillers for biphasic LM composites, as will be discussed later.

More recently, there has been exciting progress in the introduction of novel LM nanodroplet synthesis techniques and applications. This includes creation of gallium droplets in gallic acid (GA) and impregnating the GA-coated gallium particles in paper as illustrated in Fig. 1d.[24] As with previous efforts in LM sintering, pressure was used to fuse the Ga nanodroplets together to create a conductive paper composite with 1.5×10^2 S cm^{-1} volumetric conductivity. In a separate study, cellulous nanofibers were sonicated with EGaIn nanodroplets that led to producing bilayer flexible films with high conductivity (up to 8.9×10^5 S m^{-1}) and different optical reflectivity on each side.[30] For this materials system, the combination of rapid solvent evaporation, nanodroplet precipitation, and presence of nanofibers caused a spontaneous coalescence of LM nanodroplets.

Lin *et al.*[25] has demonstrated rapid and facile synthesis of EGaIn nanodroplets in under 5 minutes through ultrasonic agitation of EGaIn in a mixture of water and poly(1-octadecene-*alt*-maleic anhydride) dissolved in toluene (Fig. 1e, f). Researchers have also introduced alternative methods for creating LM nanodroplets using combined ultrasonication and microfluidics[31] and droplet nebulization.[32] The latter uses ultrasonication, but for the purpose of creating nanodroplets

through the collapse of vapor cavities formed at the LM-solvent interface rather than by shear-controlled synthesis. Lastly, there has been increasing interest in utilizing LM nanodroplets for injection in blood for imaging[33] or near-infrared photothermal tumor ablation[34] as well as for nanoparticular mediated polymerization.[35,36] Although not directly related to LM nanocomposites, these applications demonstrate the extraordinary versatility of liquid metal nanoparticles and their potential for wide impact in fields ranging from polymer engineering to nanomedicine.

LM-polymer nanocomposites

Soft LM-polymer composites were initially synthesized by shear mixing of bulk LM in an uncured elastomer using a planetary centrifugal mixer.[9] LM droplets suspended in these composites are polydisperse with average size of 10 to 140 μm depending on the polymer viscosity, LM volume fraction, and other processing parameters.[12,37–40] Increasing the shear force and mechanical agitation with immersion mixer can further reduce the size of LM droplets down to 2 μm and smaller with a uniform distribution.[29] Breaking LM droplets into nanoparticles with shear mixing becomes challenging due to the dominant surface tension of LM at this scale. Recently, Pan *et al.* have successfully synthesized soft and stretchable LM-polymer nanocomposites with different droplet sizes.[12] Ultrasound sonication was utilized to first prepare LM nanodroplets with uniform size distribution and an average diameter of 100 nm (Fig. 2a). Subsequently, the nanodroplets with a small amount of solvent were uniformly dispersed in uncured polymer using a planetary mixer. This scalable manufacturing process was used to

fabricate stretchable dielectric actuators and energy harvesters with tailored LM nanostructures (Fig. 2a).

The native metallic oxide skin (*i.e.* Ga_2O_3) of LM that forms spontaneously around the droplets can be used as a nucleation site to initiate a polymerization reaction and for *in situ* functionalization of LM nanodroplets (Fig. 2b). Yan *et al.* introduced surface-initiated atom transfer radical polymerization (SI-ATRP) as a versatile synthesis method for LM-polymer nanocomposites.[41] Polymer-coated LM nanodroplets are highly stable in organic solvents, in water, and in polymer matrices at high concentrations (up to 50 wt%). Various thermoset and thermoelastic polymer brushes such as poly(methyl methacrylate) (PMMA), poly(*n*-butyl methacrylate) (PBMA), poly(2-dimethylaminoethyl methacrylate) (PDMAEMA) and poly(*n*-butyl acrylate) (PBA) were grafted from EGaIn nanodroplets using SI-ATRP. The size of LM droplets varied from ~100 nm to 1 μm for different monomers and synthetic parameters selected for ATRP reactions (Fig. 2b). Each of these polymers have different glass transition temperatures (T_g) and elastic moduli suitable for fabrication of LM-polymer nanocomposites with tunable structural and functional properties.[29,41,42]

Atom transfer radical polymerization (ATRP) is one of the most powerful and robust controlled/living radical polymerization (CRP) techniques.[43] In ATRP, radicals are intermittently converted to dormant species to diminish contribution of radical termination. The dormant species, typically alkyl halides, are reversibly activated by low-oxidation state transition metal complexes (typically Cu^I with N-based ligand), to form propagating radicals. The radicals are quickly (after a few ms) deactivated by higher-oxidation state transition metal complexes ($X–Cu^{II}$) to re-generate the dormant chain ends.
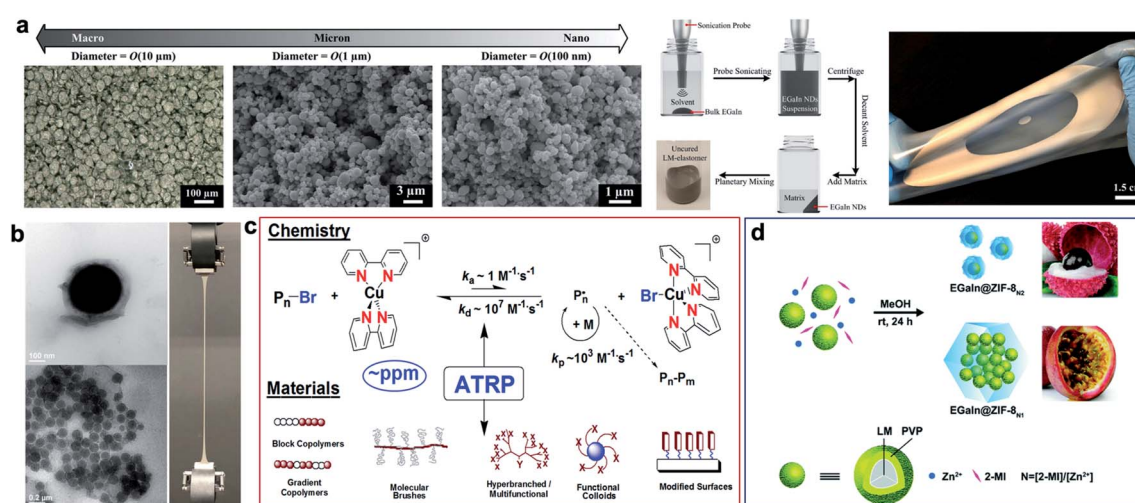

Fig. 2 Synthesis of LM-polymer composites. (a) Left: microscopic images of EGaIn micro/nanodroplets with diameter of $O(10\ \mu m)$, $O(1\ \mu m)$, and $O(100\ nm)$. The far left image presents the top view of a composite with an elastomer matrix and $O(10\ \mu m)$ droplets made by shear mixing bulk EGaIn with elastomer. Center: schematic shows the preparation of LM-nanocomposites. Right: image of stretched LM−elastomer nanocomposite (silver; annular shape) on a silicone elastomer carrier film (semitransparent). Reproduced with permission,[12] copyright 2019, Wiley-VCH. (b) LM-nanocomposites prepared by surface-initiated atom transfer radical polymerization. Reproduced with permission,[41] copyright 2019, Nature Publishing Group. (c) Schematic illustration of atom transfer radical polymerization (ATRP) and materials made by this technique. (d) Schematic illustration of the synthesis of "litchi"- and "passion fruit"-like EGaIn@ZIF-8 NPs. Pre-synthesized EGaIn@PVP nanodroplets are mixed with 2-methylimidazole (2-MI) and Zn^{2+} at different L/M ratios ($N = 2$ and 1). Reproduced with permission,[49] copyright 2020, Royal Society of Chemistry.

Equilibrium between dormant and growing species is strongly shifted to the side of dormant species as shown in Fig. 2c.[44] New ATRP techniques allow use of strongly diminished amounts of Cu-based catalysts (to a few parts per million) in the presence of environmentally friendly reducing agents.[45] The bottom part of Fig. 2c illustrates some polymeric materials prepared by ATRP.[46] They include block and gradient copolymers, molecular brushes, hyperbranched and multifunctional polymers, modified surfaces and functionalized nanoparticles. First initiators are attached to the surface of substrates and then in the presence of catalysts dense brushes (up to 1 chain per nm^2) can be grown from the inorganic surfaces.[47] The application of surface-initiated polymerization to stabilize LM nanodroplets enabled the fabrication of nanocomposites by direct assembly of polymer-modified LM nanodroplets.[41] This 'one-component' approach to composite material fabrication fundamentally differs from the established mixing or dispersion of binary (matrix/LM filler) systems in that phase separation of components is inhibited. In a similar approach but without any molecular initiator, the sonication of LMs in an aqueous solution of vinyl monomers was used to generate LM nanodroplets (∼100 nm) with grafted polymers.[36] It is postulated that LM nanoparticles serve as an initiator for free radical polymerization of vinyl-based monomers such as acrylamide. This implies LM droplets are chemically active and can be used to promote new chemical reactions. Another example of this is a study by Chang *et al.* where they synthesize 1D coordination polymers by *in situ* etching of zerovalent metal particle precursors.[48]

Another class of polymer coated LM nanodroplets was recently introduced for the growth of metal–organic frameworks (MOFs).[49] An aqueous solution of poly(*N*-vinyl-pyrrolidone) (PVP) and EGaIn were sonicated to form PVP coated LM nanodroplets (Fig. 2d). Presence of PVP stabilized LM nanodroplets, reduced the size of droplets down to 23.7 nm, and most importantly allowed growth of zeolitic imidazolate frameworks (ZIFs). Size and configuration of ZIF-encapsulated EGaIn nanoparticles can be simply controlled by varying the ligand to metal ion ratio. Enhanced photothermal response was observed from ZIF–EGaIn nanocomposites regardless of detachment of PVP coating due to high temperature of light irritation.[49] In addition.

Similar to other nanomaterials, confinement of LM droplets to nanoscale influences their thermal stability and crystallization temperature which opens up new possibilities for soft LM composites as low-temperature wearables.[29,50] In a systematic study, it was shown that independent of presence of coating, the choice of polymer matrix, and processing conditions EGaIn micro-/nanodroplets show significantly enhanced supercooling effect.[29] Their freezing temperature suppressed to −84.1 °C from −5.9 °C and their melting point reduced to −25.6 °C from +17.8 °C based on calorimetric measurements and dynamic mechanical analysis. Similar supercooling effect was observed for eutectic Ga–In–Sn nanodroplets and it was shown the superconducting properties remain nearly constant at low temperatures.[50] Comparable solidification and melting phase change behavior were also observed for Galinstan where Galinstan-PDMS composites remain soft and flexible at lower

temperatures (below −20 °C) compared to bulk Galinstan.[51] The supercooling effect was initially observed for pure Ga and Ga-based nanoparticles and elucidated by the coexistence of liquid and solid phase.[14,52,53] The supercooling effect limits the application of LM nanodroplets in composites with stiffness tuning capability as solid–liquid phase transition occurs at extremely low temperature. Unlike LM nanodroplets, phase transition of micro-/macroscale LM droplets[54–57] and fluidic channels[58–60] have been be used for rigidity tuning and shape morphing with potential applications in soft robotics.[6,61]

In recent years, LM nanodroplets have been used as stretchable conductors in emerging electronics. Nanoscale superconductors composed of Ga–In–Sn alloys were introduced by Ren *et al.* in 2016.[50] Nanosized LM droplets with thiol ligands were used as conductors in the printed flexible circuits using inkjet printing, laser lithography, and handwriting. Similar to LM-polymer composites with microdroplets, mechanical sintering is required to rupture the oxide skin and make the composites electrically conductive. Alternatively, freezing can be utilized for activation of printed LM-polymer composites.[62] Crystalized LM droplets at low temperature expand and consequently diffuse together to form a percolating network (Fig. 3a, b). Utilizing solid–liquid phase transition of LMs to compress inclusions and induce conductivity have led to development of "electrical switch" controlled by temperature.[39,63] At low temperatures, LM droplets solidify, expand, and compressed against adjacent particles to form a conductive network in the polymer matrix. When the temperature increases, LM droplets shrink and composite show significantly high electrical resistance like an insulator. Unlike mechanical and laser sintering of LM particles, this activation of LM nanodroplets is reversible, but it is restricted to composites with micron-sized LM droplets.[63]

Ultrasonication of bulk EGaIn in chloroform-hydrochloric acid with 1 to 0.01 ratio and varied sonication durations forms LM droplets with average particles sizes of 600 nm to 1.28 μm.[64] If these LM micro-/nanodroplets are shear mixed with a low weight fraction (≈0.6 wt%) of graphene flakes within elastomer medium and press-rolled, robust electrically conductive flexible composites can be fabricated. They show self-healing behavior and stable conductivity even under relatively high mechanical pressure because of the "worked" LM-graphene co-fillers.

Potential applications of LM-polymer composites have been explored in many studies leading to innovations in the thriving field of printed stretchable electronics.[4] The unique properties of LM nanodroplets can potentially further expand these application domains. For instance, nanoscale LM inclusions are capable of enhancing the dielectric properties of elastomers without significantly degrading their breakdown strength.[12] This leads to the development of soft and stretchable dielectric actuators and energy harvesters with largely enhanced electro-technical performance (Fig. 3c).[12,65] Another advantage of nanosized LM droplets is the suppression of freezing temperature. Tailored LM-polymer nanocomposites that remain soft at low temperatures (down to −80 °C), yet show high thermal conductivity, are suitable for thermoelectric energy
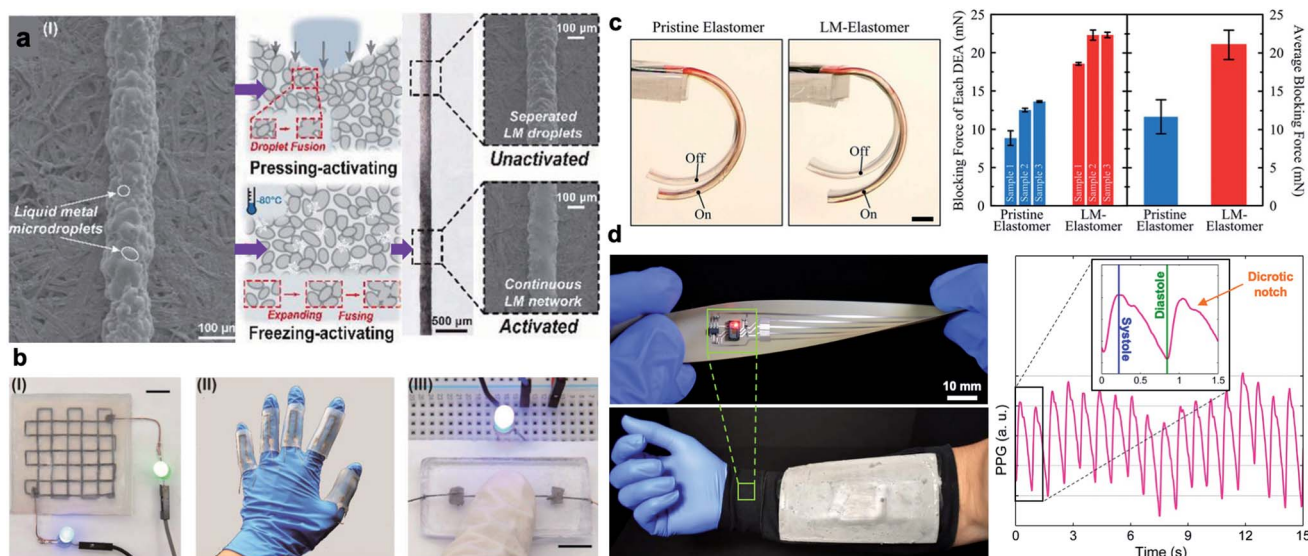
Fig. 3 Application of LM–polymer composites. (a) Left: SEM image of inactivated LM-composite ink. Center: schematic diagrams of the principle of pressing activation and freezing activation. Right: optical and SEM images of inactivated and activated LMS inks. In the SEM images, after activation, the separated LM microdroplets are sintered to a continuous LM network. Reproduced with permission,[62] copyright 2020, Wiley-VCH. (b) Potential applications in (I) multilayer circuits, (II) soft sensors, and (III) pressing-on switch (scale bar is 8 mm). Reproduced with permission,[62] copyright 2020, Wiley-VCH. (c) Image of one actuation cycle of dielectric elastomer actuators (DEAs) with unfilled elastomer as reference and LM−elastomer nanocomposite. The DEA with LM−elastomer achieves more significant actuation than unfilled elastomer (scale bar is 5 mm). Right: blocking force of DEAs. Reproduced with permission,[12] copyright 2019, Wiley-VCH. (d) Left: an implementation of a wearable pulse oximeter circuit interfaced with a hybrid thermoelectric generator (TEG) for health monitoring in extreme cold weathers. Right: a representative photoplethysmogram (PPG) waveform collected from the self-powered pulse oximetry circuit (inset: detected common features of a cardiac cycle). Reproduced with permission,[29] copyright 2019, Wiley-VCH.

harvesting.[29] This family of cold-resistant nanocomposites is used in the development of self-powered *bioelectronic sleeve* capable of monitoring individual's heart rate in cold weather conditions as shown in Fig. 3d.[29] This result indicates that LM-polymer nanocomposites with high thermal stability can be potentially used in wide range of technologies from aerospace engineering to healthcare and medical applications.

Biphasic LM-metal nanoparticle composites

Doping metallic elements into the oxide shell or the liquid core of LM droplets enables formation of biphasic LM-based composites with new functionalities and enhanced properties. For instance, deposition of a solid metallic layer (*i.e.* Au and Ag) on the outer layer of LM droplets forms a core–shell biphasic LM composite. Regardless of initial research efforts such as galvanic replacement reaction, the biphasic Au and Ag coated LM droplets were formed in irregular nanostructures and were not able to retain their shape over time at small scale.[71] David and Miki recently introduced a controllable process for synthesis of Au-encapsulated LM submicron droplets.[66] This was accomplished by separating the sonication step from galvanic reaction. As result, individual spherical LM droplets coated with a thin layer of Au or bimetallic $AuGa_2$ nanoparticles were obtained (Fig. 4a). The new biphasic LM–Au composites showed structural stability over time and can be mechanically sintered to from conductive traces for flexible circuits.

Alternatively, rigid metallic particles such as Au, Ag, Cu, Fe, Ni, and W can be mixed with liquid phase Ga-based alloys to form "paste-like" biphasic inks for printed stretchable electronics and emerging devices.[7] Liu's group have introduced various biphasic LM-metal composites aiming for enhanced thermal, electrical, and mechanical properties.[67] Semiliquid/semisolid composites with copper, gallium, and indium elements show a high electrical conductivity of 6×10^6 S m^{-1} and thermal conductivity of 50 W m^{-1} K^{-1}. Moreover, their rheological properties make them suitable for printed fine electrical circuits with a strong bonding to print substrates (Fig. 4b). More recently, biphasic LM-tungsten composites (LM-W) were synthesized to enhance the wettability and thermal conductivity of LM-based functional materials.[72] Despite the resistance of tungsten to form alloys with Ga-based LM at room temperature, tungsten powder (12 μm in diameter) was successfully mixed with LM in oxygen-rich environments. The biphasic LM-W composites were chemically stable at room temperature and could be used as thermal interface due to the integration of rigid particles of tungsten with a thermal conductivity of 173 W m^{-1} K^{-1}. The highest level of thermal conductivity was achieved for 40% volume fraction of tungsten with a two-to threefold enhancement in thermal conductivity (2 ± 2.28 W m^{-1} K^{-1} for Ga and 57 ± 2.08 W m^{-1} K^{-1} for EGaInSn). Another family of biphasic composites named "GIN" was synthesized by low speed shear mixing of nickel (Ni) powder (∼20% mass fraction) in bulk EGaIn.[73] Compared to pure LM, biphasic GIN shows superior wettability and strong adhesion to

Fig. 4 Biphasic LM-composites for epidermal applications. (a) SEM images of deposited $AuGa_2$-LM and Au-LM after galvanic replacement with 1 and 10 mM $KAuBr_4$–KOH. Reproduced with permission,[66] copyright 2019, Royal Society of Chemistry. (b) Left: schematic of the particles inside liquid metal. Left-inset: rugged surface of biphasic LM-composite (top view), Right-inset: liquid bridges formed between solid particles (cross-sectional view). Reproduced with permission,[67] copyright 2017, American Society of Chemistry. (c) Top: the Ni-EGaIn electronic tattoo heater designed in a variety of shapes with various heating effects. Middle: schematic and photo of Ni-EGaIn electronic tattoo electrodes with poly-methacrylate (PMA) interface. Bottom: a 3-electrode EMG recordings printed on the forearm of a healthy volunteer along with the EMG recordings under different hand gestures. Reproduced with permission,[68] copyright 2019, Wiley-VCH. (d) Top: stretchable biphasic conductor formed by physical vapor deposition of gallium onto an alloying metal film. Bottom: soft optoelectronic assembly and transducers enabled by intrinsically stretchable biphasic metallization. Bottom left: photo showing the soft matrix of microheaters wrapped on a human arm. Temperature gradients along the x-axis are indicated by the blue arrow. Bottom right: infrared images of a 3×3 matrix of microheaters on the human forearm while sequentially heating one row after the other (scale bars are 10 mm except for zoomed microheater picture is 1 mm). Reproduced with permission,[69] copyright 2016, Wiley-VCH. (e) Soft, stretchable, and ultrathin printed electronic tattoos prepared by EGaIn-assisted room-temperature sintering of silver nanoparticles. Top: transferred electronic tattoo to human fingertip. Bottom: the printed biphasic conductors transferred to the highly textured surface of a toy brain. Reproduced with permission,[70] copyright 2018, Wiley-VCH.

paper making them suitable for direct-writing of paper-based flexible electronics.

In addition to enhanced thermal conductivity, semisolid LM–Ni composites show high electrical conductivity and large deformability when deposited on elastomer substrate (*i.e.* Ecoflex). For EGaIn–Ni composites with 15% mass fraction of Ni microparticles, a high conductivity of $\sim 1.6 \times 10^6$ S m^{-1} was reported.[74] Printing LM–Ni composites with rolling brush has being used for fabrication of wireless healthcare wearables embedded in layers of Ecoflex. In a follow-up study, the elastomeric substrate was replaced by polymethacrylate (PMA) glue to allow direct transfer of EGaIn–Ni conductive ink to human skin.[68] Various epidermal electronics such as LED arrays, heaters, and temperature sensors were fabricated using this fabrication method (Fig. 4c).

Noble metals such as Au and Ag can be used as a wetting/ alloying template to create biphasic LM composites for high-resolution printed electronics. Intrinsically stretchable Ga-

based biphasic conductors were initially introduced by Hirsch *et al.*[69] To prepare the solid–liquid film conductors, liquid Ga was evaporated on an elastomer substrate with a patterned wetting/alloying film. Using sputtered Au as the alloying film overcame the high surface tension of LM and formed a continuous conductive network while evaporated Ga did not bond to bare elastomer surfaces (Fig. 4d – top). After optimizing the Au/ Ga ratio, epidermal flexion sensor skin and soft wearable microheaters were fabricated by these biphasic LM films (Fig. 4d-bottom). Later, inkjet-printed Ag nanoparticles were utilized an alternative alloying pattern by Tavakoli *et al.*[70,75] A thin layer of EGaIn was deposited on Ag nanoparticles printed on a temporary tattoo paper to create ultrathin stretchable conductors for skin-like electronics termed "electronic tattoo".[70] Room-temperature sintered Ag nanoparticles form a new biphasic LM-Ag alloy with high electrical conductivity ($\sim 4.8 \times 10^6$ S m^{-1}) and large maximum failure strain (up to 120%) when coated with elastomer. In addition, the low-cost, scalable,

practical fabrication process of LM-Ag composites facilitate fabrication of various electronic skins transferable to human body or objects with complex 3D geometry (Fig. 4e). It should be mentioned that most printed biphasic LM-metal conductors can be interfaced with rigid microelectronic chips and processors through liquid metal soldering.[76]

Integration of magnetic particles such as Fe and Ni into liquid metals has untapped new functions for LM-based systems. For instance, gadolinium (Gd) can be dissolved in Galinstan to create precipitated Gd nanoparticles (up to 2%) within LM.[77] This process results in LM-based ferrofluid that demonstrate macroscopic magnetic properties and can be used for magnetocaloric refrigeration. More recently, bulk EGaIn and Fe particles were mixed in HCl solution in order to create LM foam responsive to external magnetic fields.[78] In a similar approach, Galinstan was mixed with Fe particles to be used as a magnetoactive paste for adaptive bioelectrodes (Fig. 5a). Reversible stiffness tuning within the kPa to MPa range (factor of 1000) was reported for this class of Galinstan–Fe composites.[79] Potential applications of this novel magnetoactive composite was demonstrated by fabrication of soft implanted electrodes or penetrating bioelectrodes that can be controlled

with external magnetic field. In general, LM-based magnetic materials have a great potential as actuators in soft robotics.[80] Another innovative application of magnetically responsive LM-composites is in magnetic-assisted direct-writing of stretchable electronics.[81] In this versatile manufacturing technique, the liquid core of LM droplets acts as the ink and also a carrier of Ni magnetic particles. When a magnetic field is applied through a substrate, Ni particles aggregate and enable remote manipulation of ink resulting in direct patterning of LMs on variety of substrates (Fig. 5b).

Outlook & future work

Research in liquid metal nanocomposites and nanodroplet systems is still in its nascent stages, with tremendous opportunities for continued scientific advancements and technological impact. The work reported here represents early efforts to synthesize LM nanomaterial systems and characterize their elastic, rheological, electrical, thermal, and electromagnetic properties. Further progress will depend on methods that can precisely control the average size, size distribution, and yield of LM nanodroplets with a wide variety of surfactants, polymer coatings, and dispersion media.

As these methods are further refined, there will be an increasing need for theoretical models and computational tools that aid in the design of LM nanocomposites with target material properties. Using a computational method based on fast Fourier transform, Dehnavi et al.[82] showed predictions for the increase in thermal conductivity of LM-polymer composites as a function of LM droplet volume fraction that were in good agreement with experimental measurements made by Tutika et al.[83] Recently, Cohen & Bhattacharya introduced a model based on finite element analysis to predict the electromechanical coupling of electrically conductive LM-embedded elastomer composites.[84] Although further work is required to show agreement with experimental measurements, this model does make predictions that are consistent with experimental observations that the change in electrical resistance with stretch is dependent on the spatial distribution of the percolating network of droplets.

Future efforts should also address challenges with interfacing LM nanocomposites with other materials and functional elements. For example, as shown in Fig. 4e, applications in thin-film and stretchable electronics typically require surface-mounted microelectronic components. The electrical connections formed between conductive LM nanomaterials and the pins of these packaged microelectronics must be robust and remain electrically stable under mechanical loading. Another challenge that needs to be addressed is the corrosion and embrittlement of metals (i.e. aluminum and copper) induced by Ga-based alloys. It has been illustrated that surface modified LM nanodroplets show stable anti-corrosion effect (even in direct contact with aluminum).[85] While the LM nanodroplets possess high thermal conductivity, they become electrically insulating. Likewise, efforts to use biphasic LM-metal nanomaterials for thermal management in computing devices should also address issues related to thermal contact resistance
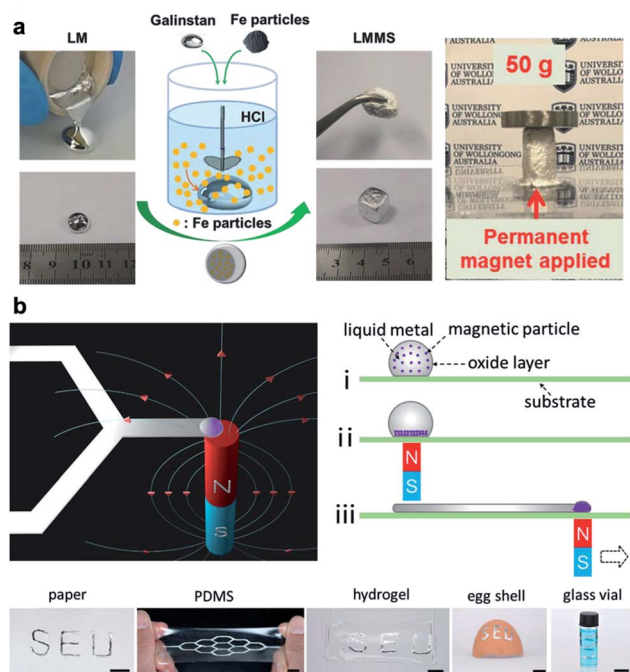

Fig. 5 Magnetically responsive LM-composites. (a) Left: schematic illustration and photographs demonstrating the preparation of LM-based magnetoactive slurries (LMMS). The liquid Galinstan becomes slurry-like after mixing with the Fe particles in the HCl solution. Right: a cylindrical shape molded under the field from a permanent magnet showing no deformation under a 50 g weight. Reproduced with permission,[79] Copyright 2018, Wiley-VCH. (b) Top-left: illustration of the direct patterning of LM using magnetic field. Top-right: detailed operation steps for liquid metal patterning. Bottom: photographs of LM patterns on different substrates including planar substrates and curved surfaces of an eggshell and the inner wall of the glass vial (scale bars are 10 mm). Reproduced with permission,[81] copyright 2019, Wiley-VCH.

and intermetallic alloying or corrosion. As LM nanocomposites and nanodroplet systems find widening applications in electronics, medicine, and soft robotics over the forthcoming years, new sets of target properties and metrics of performance will emerge. Addressing these will depend on continued advancements in LM nanomaterial synthesis and design at the intersection of chemistry, polymer engineering, computational modeling, and nanotechnology.

Conflicts of interest

There are no conflicts to declare.

Acknowledgements

References

1 T. Daeneke, K. Khoshmanesh, N. Mahmood, I. De Castro, D. Esrafilzadeh, S. Barrow, M. Dickey and K. Kalantar-Zadeh, *Chem. Soc. Rev.*, 2018, **47**, 4073–4111.

2 M. D. Dickey, *Adv. Mater.*, 2017, **29**, 1606425.

3 T. Kim, D. Kim, B. J. Lee and J. Lee, *Sensors*, 2019, **19**, 4250.

4 L. Zhu, B. Wang, S. Handschuh-Wang and X. Zhou, *Small*, 2019, **16**, 1903841.

5 T. Gan, W. Shang, S. Handschuh-Wang and X. Zhou, *Small*, 2019, **15**, 1804838.

6 L. Ren, X. Xu, Y. Du, K. Kalantar-Zadeh and S. X. Dou, *Mater. Today*, 2019, DOI: 10.1016/j.mattod.2019.10.007.

7 M. Zhang, S. Yao, W. Rao and J. Liu, *Mater. Sci. Eng., R*, 2019, **138**, 1–35.

8 Y. Lu, Q. Hu, Y. Lin, D. B. Pacardo, C. Wang, W. Sun, F. S. Ligler, M. D. Dickey and Z. Gu, *Nat. Commun.*, 2015, **6**, 1–10.

9 N. Kazem, T. Hellebrekers and C. Majidi, *Adv. Mater.*, 2017, **29**, 1605985.

10 H. Song, T. Kim, S. Kang, H. Jin, K. Lee and H. J. Yoon, *Small*, 2019, 1903391.

11 K. Kalantar-Zadeh, J. Tang, T. Daeneke, A. P. O'Mullane, L. A. Stewart, J. Liu, C. Majidi, R. S. Ruoff, P. S. Weiss and M. D. Dickey, *ACS Nano*, 2019, **13**, 7388–7395.

12 C. Pan, E. J. Markvicka, M. H. Malakooti, J. Yan, L. Hu, K. Matyjaszewski and C. Majidi, *Adv. Mater.*, 2019, **31**, 1900663.

13 J. N. Hohman, M. Kim, G. A. Wadsworth, H. R. Bednar, J. Jiang, M. A. LeThai and P. S. Weiss, *Nano Lett.*, 2011, **11**, 5104–5110.

14 A. Yamaguchi, Y. Mashima and T. Iyoda, *Angew. Chem., Int. Ed.*, 2015, **54**, 12809–12813.

15 J. W. Boley, E. L. White and R. K. Kramer, *Adv. Mater.*, 2015, **27**, 2355–2360.

16 Y. Lin, C. Cooper, M. Wang, J. J. Adams, J. Genzer and M. D. Dickey, *Small*, 2015, **11**, 6397–6403.

17 S. Liu, M. C. Yuen, E. L. White, J. W. Boley, B. Deng, G. J. Cheng and R. Kramer-Bottiglio, *ACS Appl. Mater. Interfaces*, 2018, **10**, 28232–28241.

18 B. Deng and G. J. Cheng, *Adv. Mater.*, 2019, **31**, 1807811.

19 L. R. Finkenauer, Q. Lu, I. F. Hakem, C. Majidi and M. R. Bockstaller, *Langmuir*, 2017, **33**, 9703–9710.

20 Z. J. Farrell and C. Tabor, *Langmuir*, 2018, **34**, 234–240.

21 N. J. Morris, Z. J. Farrell and C. E. Tabor, *Nanoscale*, 2019, **11**, 17308–17318.

22 J. Cutinho, B. S. Chang, S. Oyola-Reynoso, J. Chen, S. S. Akhter, I. D. Tevis, N. J. Bello, A. Martin, M. C. Foster and M. M. Thuo, *ACS Nano*, 2018, **12**, 4744–4753.

23 A. Martin, W. Kiarie, B. Chang and M. Thuo, *Angew. Chem., Int. Ed.*, 2020, **59**, 352–357.

24 F. Centurion, M. G. Saborío, F. Allioux, S. Cai, M. B. Ghasemian, K. Kalantar-Zadeh and M. A. Rahim, *Chem. Commun.*, 2019, **55**, 11291–11294.

25 Y. Lin, J. Genzer, W. Li, R. Qiao, M. D. Dickey and S. Tang, *Nanoscale*, 2018, **10**, 19871–19878.

26 I. D. Tevis, L. B. Newcomb and M. Thuo, *Langmuir*, 2014, **30**, 14308–14313.

27 S. Çinar, I. D. Tevis, J. Chen and M. Thuo, *Sci. Rep.*, 2016, **6**, 1–12.

28 A. Martin, B. S. Chang, Z. Martin, D. Paramanik, C. Frankiewicz, S. Kundu, I. D. Tevis and M. Thuo, *Adv. Funct. Mater.*, 2019, **29**, 1903687.

29 M. H. Malakooti, N. Kazem, J. Yan, C. Pan, E. J. Markvicka, K. Matyjaszewski and C. Majidi, *Adv. Funct. Mater.*, 2019, **29**, 1906098.

30 X. Li, M. Li, J. Xu, J. You, Z. Yang and C. Li, *Nat. Commun.*, 2019, **10**, 1–9.

31 S. Tang, R. Qiao, S. Yan, D. Yuan, Q. Zhao, G. Yun, T. P. Davis and W. Li, *Small*, 2018, **14**, 1800118.

32 S. Tang, R. Qiao, Y. Lin, Y. Li, Q. Zhao, D. Yuan, G. Yun, J. Guo, M. D. Dickey and T. J. Huang, *Adv. Mater. Technol.*, 2019, **4**, 1800420.

33 X. Huang, J. Hu, Y. Li, F. Xin, R. Qiao and T. P. Davis, *Biomacromolecules*, 2019, **20**, 4243–4257.

34 P. Zhu, S. Gao, H. Lin, X. Lu, B. Yang, L. Zhang, Y. Chen and J. Shi, *Nano Lett.*, 2019, **19**, 2128–2137.

35 T. Gan, S. Handschuh-Wang, W. Shang, J. Shen, L. Zhu, Q. Xiao, S. Hu and X. Zhou, *Macromol. Rapid Commun.*, 2019, **40**, 1900537.

36 J. Ma, Y. Lin, Y. Kim, Y. Ko, J. Kim, K. H. Oh, J. Sun, C. B. Gorman, M. A. Voinov and A. I. Smirnov, *ACS Macro Lett.*, 2019, **8**, 1522–1527.

37 L. Zhu, Y. Chen, W. Shang, S. Handschuh-Wang, X. Zhou, T. Gan, Q. Wu, Y. Liu and X. Zhou, *J. Mater. Chem. C*, 2019, **7**, 10166–10172.

38 E. J. Markvicka, M. D. Bartlett, X. Huang and C. Majidi, *Nat. Mater.*, 2018, **17**, 618–624.

39 H. Wang, Y. Yao, Z. He, W. Rao, L. Hu, S. Chen, J. Lin, J. Gao, P. Zhang and X. Sun, *Adv. Mater.*, 2019, **31**, 1901337.

40 R. Tutika, S. Kmiec, A. T. Haque, S. W. Martin and M. D. Bartlett, *ACS Appl. Mater. Interfaces*, 2019, **11**, 17873–17883.

41 J. Yan, M. H. Malakooti, Z. Lu, Z. Wang, N. Kazem, C. Pan, M. R. Bockstaller, C. Majidi and K. Matyjaszewski, *Nat. Nanotechnol.*, 2019, **14**, 684–690.

42 J. Yan, M. R. Bockstaller and K. Matyjaszewski, *Prog. Polym. Sci.*, 2019, **100**, 101180.

43 J. Wang and K. Matyjaszewski, *J. Am. Chem. Soc.*, 1995, **117**, 5614–5615.

44 T. E. Patten, J. Xia, T. Abernathy and K. Matyjaszewski, *Science*, 1996, **272**, 866–868, DOI: 10.1126/science.272.5263.866.

45 N. V. Tsarevsky and K. Matyjaszewski, *Chem. Rev.*, 2007, **107**, 2270–2299.

46 K. Matyjaszewski, *Adv. Mater.*, 2018, **30**, 1706441.

47 C. M. Hui, J. Pietrasik, M. Schmitt, C. Mahoney, J. Choi, M. R. Bockstaller and K. Matyjaszewski, *Chem. Mater.*, 2014, **26**, 745–762.

48 B. S. Chang, B. Thomas, J. Chen, I. D. Tevis, P. Karanja, S. Çinar, A. Venkatesh, A. J. Rossini and M. M. Thuo, *Nanoscale*, 2019, **11**, 14060–14069.

49 Y. Liu, Q. Wang, J. Deng and W. Zhang, *Chem. Commun.*, 2020, **56**, 1851–1854.

50 L. Ren, J. Zhuang, G. Casillas, H. Feng, Y. Liu, X. Xu, Y. Liu, J. Chen, Y. Du and L. Jiang, *Adv. Funct. Mater.*, 2016, **26**, 8111–8118.

51 A. Koh, W. Hwang, P. Y. Zavalij, S. Chun, G. Slipher and R. Mrozek, *Materialia*, 2019, **8**, 100512.

52 S. Tang, D. R. Mitchell, Q. Zhao, D. Yuan, G. Yun, Y. Zhang, R. Qiao, Y. Lin, M. D. Dickey and W. Li, *Matter*, 2019, **1**, 192–204.

53 M. Losurdo, A. Suvorova, S. Rubanov, K. Hingerl and A. S. Brown, *Nat. Mater.*, 2016, **15**, 995.

54 I. M. Van Meerbeek, B. C. Mac Murray, J. W. Kim, S. S. Robinson, P. X. Zou, M. N. Silberstein and R. F. Shepherd, *Adv. Mater.*, 2016, **28**, 2801–2806.

55 B. S. Chang, R. Tutika, J. Cutinho, S. Oyola-Reynoso, J. Chen, M. D. Bartlett and M. M. Thuo, *Mater. Horiz.*, 2018, **5**, 416–422.

56 T. L. Buckner, M. C. Yuen, S. Y. Kim and R. Kramer-Bottiglio, *Adv. Funct. Mater.*, 2019, **29**, 1903368.

57 W. Shan, T. Lu and C. Majidi, *Smart Mater. Struct.*, 2013, **22**, 085005.

58 A. Tonazzini, S. Mintchev, B. Schubert, B. Mazzolai, J. Shintake and D. Floreano, *Adv. Mater.*, 2016, **28**, 10142–10148.

59 R. Takahashi, T. L. Sun, Y. Saruwatari, T. Kurokawa, D. R. King and J. P. Gong, *Adv. Mater.*, 2018, **30**, 1706885.

60 F. Deng, Q. Nguyen and P. Zhang, *Addit. Manuf.*, 2020, **33**, 101117.

61 L. Wang, Y. Yang, Y. Chen, C. Majidi, F. Iida, E. Askounis and Q. Pei, *Mater. Today*, 2018, **21**, 563–576.

62 L. Zhou, J. Fu, Q. Gao, P. Zhao and Y. He, *Adv. Funct. Mater.*, 2020, **30**, 1906683.

63 S. Chen, H. Wang, X. Sun, Q. Wang, X. Wang, L. Chen, L. Zhang, R. Guo and J. Liu, *Mater. Horiz.*, 2019, **6**, 1854–1861.

64 M. G. Saborio, S. Cai, J. Tang, M. B. Ghasemian, M. Mayyas, J. Han, M. J. Christoe, S. Peng, P. Koshy and D. Esrafilzadeh, *Small*, 2019, 1903753.

65 Y. Wang, G. Sun, J. Yang, L. Zhang and J. Zhou, *AIP Adv.*, 2020, **10**, 015016.

66 R. David and N. Miki, *Nanoscale*, 2019, **11**, 21419–21432.

67 J. Tang, X. Zhao, J. Li, R. Guo, Y. Zhou and J. Liu, *ACS Appl. Mater. Interfaces*, 2017, **9**, 35977–35987.

68 R. Guo, X. Sun, S. Yao, M. Duan, H. Wang, J. Liu and Z. Deng, *Adv. Mater. Technol.*, 2019, **4**, 1900183.

69 A. Hirsch, H. O. Michaud, A. P. Gerratt, S. De Mulatier and S. P. Lacour, *Adv. Mater.*, 2016, **28**, 4507–4512.

70 M. Tavakoli, M. H. Malakooti, H. Paisana, Y. Ohm, D. Green Marques, P. Alhais Lopes, A. P. Piedade, A. T. de Almeida and C. Majidi, *Adv. Mater.*, 2018, **30**, 1801852.

71 F. Hoshyargar, J. Crawford and A. P. O'Mullane, *J. Am. Chem. Soc.*, 2017, **139**, 1464–1471.

72 W. Kong, Z. Wang, M. Wang, K. C. Manning, A. Uppal, M. D. Green, R. Y. Wang and K. Rykaczewski, *Adv. Mater.*, 2019, **31**, 1904309.

73 H. Chang, R. Guo, Z. Sun, H. Wang, Y. Hou, Q. Wang, W. Rao and J. Liu, *Adv. Mater. Interfaces*, 2018, **5**, 1800571.

74 R. Guo, X. Wang, H. Chang, W. Yu, S. Liang, W. Rao and J. Liu, *Adv. Eng. Mater.*, 2018, **20**, 1800054.

75 P. A. Lopes, H. Paisana, A. T. De Almeida, C. Majidi and M. Tavakoli, *ACS Appl. Mater. Interfaces*, 2018, **10**, 38760–38768.

76 K. B. Ozutemiz, J. Wissman, B. Ozdoganlar and C. Majidi, *Adv. Mater. Interfaces*, 2018, **5**, 1701596.

77 I. A. de Castro, A. F. Chrimes, A. Zavabeti, K. J. Berean, B. J. Carey, J. Zhuang, Y. Du, S. X. Dou, K. Suzuki and R. A. Shanks, *Nano Lett.*, 2017, **17**, 7831–7838.

78 H. Wang, B. Yuan, S. Liang, R. Guo, W. Rao, X. Wang, H. Chang, Y. Ding, J. Liu and L. Wang, *Mater. Horiz.*, 2018, **5**, 222–229.

79 L. Ren, S. Sun, G. Casillas-Garcia, M. Nancarrow, G. Peleckis, M. Turdy, K. Du, X. Xu, W. Li and L. Jiang, *Adv. Mater.*, 2018, **30**, 1802595.

80 X. Wang, R. Guo and J. Liu, *Adv. Mater. Technol.*, 2019, **4**, 1800549.

81 B. Ma, C. Xu, J. Chi, J. Chen, C. Zhao and H. Liu, *Adv. Funct. Mater.*, 2019, **29**, 1901370.

82 F. N. Dehnavi, M. Safdari, K. Abrinia, A. Sheidaei and M. Baniassadi, *Mater. Today Commun.*, 2020, **23**, 100878.

83 R. Tutika, S. H. Zhou, R. E. Napolitano and M. D. Bartlett, *Adv. Funct. Mater.*, 2018, **28**, 1804336.

84 N. Cohen and K. Bhattacharya, *Int. J. Non Lin. Mech.*, 2019, **108**, 81–86.

85 P. Fan, Z. Sun, Y. Wang, H. Chang, P. Zhang, S. Yao, C. Lu, W. Rao and J. Liu, *RSC Adv.*, 2018, **8**, 16232–16242.